

Needle placement accuracy in MRI-guided prostate biopsy of prostate cancer

N. Hata¹, P. Blumenfeld¹, S. DiMaio¹, K. Zou¹, S. Haker¹, C. M. Tempany¹

¹Radiology, Brigham and Women's Hospital and Harvard Medical School, Boston, MA, United States

INTRODUCTION

Magnetic Resonance Image-guided prostate biopsy provides an alternative approach to detect and diagnose prostate cancer (1-3). The biopsies targeted at suspected tumor *foci*, observed in 1.5T and/or 0.5T pre-procedural images, are of particular merit; recent study of 53 cases (4) had cancer diagnosed in 38%. Of patients and in those 71% of the tissue diagnosed as adenocarcinoma from these sites, compared with 29% from sextant biopsy of the peripheral zone. Although the transperineal MR-guided biopsy has improved the efficacy of prostate diagnosis through high detection yields at targeted foci the accuracy of the core biopsy needle placement in transperineal procedures has never been evaluated. The purpose of this study was to assess the accuracy of needle placement during MR-guided prostate biopsies. In addition, we have developed a taxonomy of those factors that contribute to misplacement. This investigation will help to prompt further improvements in the quality of this already promising detection and diagnosis method for prostate cancer.

METHODS

First, a total of 10 randomly selected MR-guided prostate biopsy cases (patient age: 61.9 ± 4.7 years; average prostate volume 75.0 cc) were retrospectively reviewed. We measured the distances between the physician's pre-planned biopsy locations that were specified in T2-weighted Fast Spin Echo images, and the tip of the needle susceptibility artifact observed in intra-procedural FGR images used for monitoring needle placement during the cases. The errors were summarized using their mean, standard deviation (SD), and median values, stratified by location and by target versus non-target. Outliers were excluded when the z-score of the error was beyond ± 3 , where the z-score is defined as (data-mean)/(standard deviation) within each case.

Second, we designed a phantom experiment to quantify needle deflection error. Gelatin, bovine liver, and bovine muscle tissue samples were each in turn placed inside the phantom enclosure. Needles were inserted through the entry holes and phantom samples, toward the marked target points at the distal end of the enclosure. We used MR-compatible 18 gauge core biopsy needles with a symmetrical bevel (E-Z-EM, Inc., Westbury, NY), termed the symmetrical needles, and needles with an asymmetrical bevel (US Biopsy, Franklin, IN), termed the asymmetrical needles. Each of the needles was inserted 7 times into each of the 3 different tissues, while two readers used a vernier caliper to measure the resulting distance between the target point and the needle tip.

Third, we analyzed needle artifacts in phantom study which spatially shift along the frequency encoding direction(5). We quantified this artifact shift in images acquired using the 0.5T open-configuration MRI scanner, under imaging conditions identical to those used in the clinical MRI-guided biopsies described in (1,2,4). Needles were scanned while immersed in water containing a gadolinium contrast agent mixed with a ratio of 500:1. The phantom was placed in the 0.5T open-configuration scanner, with the needle oriented perpendicular to the static field (B_0) of the magnet. FGR images were acquired. The experiment was repeated for varying frequency encoding directions (Right/Left and Anterior/Posterior), and slice thicknesses (5mm and 7mm). Established clinical practice dictated the choice of these variables.

RESULTS

The mean and standard deviation of the errors in targeted biopsies was 6.5 ± 3.5 mm, with a median of 6.4mm, while for non-targeted locations the mean error was found to be 6.7 ± 4.4 mm, with a median of 6.0mm (Figure 1). A statistically significant difference was found when comparing the mean errors between targeted biopsy and non-targeted biopsy groups ($p < 0.001$). From the phantom experiments, the mean tip deflection and standard deviations measured using the asymmetrical needle were 4.6 ± 0.4 mm, 3.2 ± 0.5 mm, and 8.7 ± 0.8 mm, in gelatin, bovine liver, and bovine muscle tissue, respectively. The means and standard deviations measured when using the symmetrical biopsy needle were 0.8 ± 0.6 mm, 0.6 ± 0.6 mm, and 1.1 ± 0.5 mm for each phantom respectively (Table 1). Relatively small correlation was found among different tissue types in trials with the symmetric needle ($p = 0.23$), compared to trials with the asymmetric needle ($p < 0.0001$). The analysis of needle susceptibility artifact yielded a mean artifact shift of 1.6 ± 0.4 mm along the direction of the frequency encode direction.

DISCUSSION

The accuracy results from our study of clinical data, as well as from phantom experiments, indicate that the method is limited by the accuracy with which the needles can be placed, and that there are a number of physical factors that are significant sources of placement error. The results from our study are comparable to previous literature (6,7). However, our study further extended the assessment and showed that depending on the type of needle and its insertion depth, needle deflection can also be a major cause for error in prostate biopsies. We believe that a mechanism that can provide more accurate and flexible needle placement than the stereotactic template guide that is currently used would make MR-guided biopsies the gold standard for prostate biopsies.

In summary, we have analyzed needle placement errors in MRI-guided biopsy of prostate cancer and showed that the mean error from 10 clinical cases was 6.5mm for targeted biopsies. Phantom experiments showed that needle placement error due to needle deflection was significant when a needle with asymmetrical bevel was used. This has led us to believe that one cause of rather significant placement error, 6.5 mm, in clinical practice is needle deflection.

Table 1: Error due to needle deflection, artifact susceptibility, and template registration.

Error due to	Phantom setup	Mean (mm)	SD (mm)
Asymmetrical Needle Deflection	Gelatine	4.6	0.4
	Bovine Liver	3.2	0.5
	Bovine Muscle Tissue	8.7	0.8
Symmetrical Needle Deflection	Gelatine	0.8	0.6
	Bovine Liver	0.6	0.6
	Bovine Muscle Tissue	1.1	0.5
Artifact Susceptibility	Gadolinium; 5 mm slice; R/L freq.	1.6	0.1
	Gadolinium; 5 mm slice; A/P freq.	1.8	0.2
	Gadolinium; 7 mm slice; R/L freq.	1.7	0.4
	Gadolinium; 7 mm slice; A/P freq.	1.4	0.5

SD: Standard Deviation, R/L: Right-to-Left, A/P: Anterior-to-Posterior

REFERENCES

1. D'Amico AV, Tempany CM, Cormack R, et al. J Urol 2000;164(2):385-387.
2. Hata N, Jinzaki M, Kacher D, et al. Radiology 2001; 220:263-268
3. Zangos S, Eichler K, Engelmann K, et al. Eur Radiol 2005;15(1):174-182.
4. So MJ, Haker S, Zou KH, et al. ISMRM 2005; Miami, FL. p 264.
5. Butts K, Pauly JM, Daniel BL, et al. J Magn Reson Imaging 1999;9(4):586-595.
6. Susil RC, Camphausen K, Choyke P, et al. Magn Reson Med 2004;52(3):683-687.
7. Schneider E, Rohling KW, Schnell MD, et al. J Magn Reson Imaging 2001;14(3):243-253.

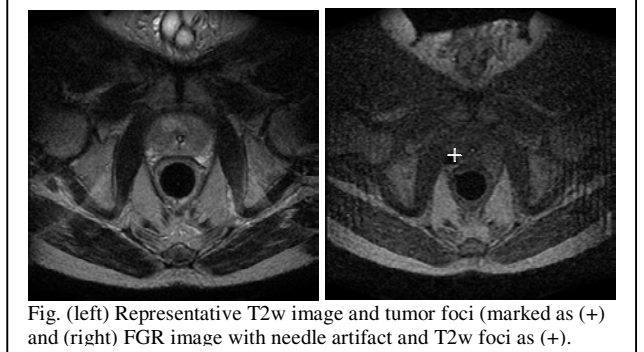


Fig. (left) Representative T2w image and tumor foci (marked as (+) and (right) FGR image with needle artifact and T2w foci as (+).